

WHO MATTERS MATTERS: AGENT-SPECIFIC CONSERVATIVE OFFLINE MARL

000
001
002
003
004
005
006
007
008
009
010
011
012
013
014
015
016
017
018
019
020
021
022
023
024
025
026
027
028
029
030
031
032
033
034
035
036
037
038
039
040
041
042
043
044
045
046
047
048
049
050
051
052
053
Anonymous authors
Paper under double-blind review

ABSTRACT

Offline Multi-Agent Reinforcement Learning (MARL) enables policy learning from static datasets in multi-agent systems, eliminating the need for risky or costly environment interactions during training. A central challenge in offline MARL lies in achieving effective collaboration among heterogeneous agents under the constraints of fixed datasets, where **conservatism** is introduced to restrict behaviors to data-supported distributions. Agents with distinct roles and capabilities require individualized conservatism - yet must maintain cohesive team performance. However, existing approaches often apply uniform conservatism across all agents, leading to over-constraining critical agents and under-constraining others, which hampers effective collaboration. To address this issue, a novel framework, **OMCDA**, is proposed, where the degree of conservatism is dynamically adjusted for individual agents based on their impact on overall system performance. The framework is characterized by two key innovations: (1) A decomposed Q-function architecture is introduced to disentangle return computation from policy deviation assessment, allowing precise evaluations of each agent’s contribution; and (2) An adaptive conservatism mechanism is developed to scale constraint strength according to both behavior policy divergence and the estimated importance of agents to the system. Experiments on MuJoCo and SMAC show OMCDA outperforms existing offline MARL methods, effectively balancing the flexibility and conservatism across agents while ensuring fair credit assignment and better collaboration.

1 INTRODUCTION

Multi-agent reinforcement learning (MARL) has gained significant traction in domains such as autonomous driving (Cao et al., 2012), collaborative robotics (Orr & Dutta, 2023), and multi-player games (Berner et al., 2019), where agents must learn to coordinate or compete to accomplish complex objectives. Despite its successes, most MARL approaches assume agents can interact freely with the environment during training. In practice, however, this assumption often breaks down due to high interaction costs, safety concerns, or operational constraints (Wang et al., 2024). To address these limitations, Offline Reinforcement Learning (Offline RL) has emerged as a compelling alternative (Fujimoto & Gu, 2021; Kostrikov et al., 2021b; Kumar et al., 2020; Levine et al., 2020; Wu et al., 2019). Instead of relying on real-time interactions, Offline RL learns from pre-collected datasets, making it more practical for safety-critical or data-scarce environments. In the single-agent setting, Offline RL has achieved notable progress by addressing challenges such as Q-value overestimation for out-of-distribution (OOD) actions, which often lead to poor generalization. A key development in this direction is the use of *conservative* methods (Wu et al., 2019), which penalize unlikely or unsupported actions to ensure that learned policies remain close to the behavior policy. This form of **conservatism** is defined as the tendency to favor actions supported by the training data while avoiding uncertain or OOD behaviors which improves stability and robustness during offline learning (Kumar et al., 2020).

When Offline RL is extended to multi-agent settings (Offline MARL), the situation becomes even more complex. The interplay among agents introduces increased non-stationarity, and the offline dataset can exhibit more severe distributional shifts. Moreover, credit assignment—how each agent’s actions contribute to overall joint performance—presents a substantial challenge (Wang & Zhan, 2023; Yang et al., 2021). Recent efforts has explored Offline MARL under the “Centralized Training

054 and Decentralized Execution” (CTDE) framework (Lowe et al., 2017), leveraging multi-agent value
 055 decomposition combined with offline conservatism to stabilize learning.
 056

057 Nevertheless, existing studies seldom consider the heterogeneity of agents in real world applications.
 058 Due to their distinct roles and interaction patterns, different agents can wield unequal influence on
 059 overall system performance (Wang et al., 2020b; Foerster et al., 2018). For instance, in a football team,
 060 strikers are often encouraged to take creative, high-risk actions to maximize scoring opportunities,
 061 while defenders must adhere to disciplined, risk-averse strategies to ensure team stability. Imposing
 062 equal conservatism on both roles would limit the striker’s effectiveness and increase the defender’s
 063 exposure to costly errors. This illustrates that the appropriate level of conservatism should depend on
 064 the agent’s role, uncertainty, and potential impact. Consequently, a central challenge in heterogeneous
 065 Offline MARL is how to *adaptively assign conservatism* across agents based on their individual
 066 characteristics—striking a balance between safety and exploration that enhances both performance
 067 and reliability so as to promote their collaboration.

068 In this study, we introduce a novel offline MARL approach, **Offline MARL with Conservative**
Degree Allocation (OMCDA), which addresses the challenge of distributing conservatism among
 069 agents based on their deviations from behavior policies and their impact on system performance
 070 for heterogeneous agents in offline MARL. OMCDA decomposes the Q-function in offline MARL
 071 with regularization into two components: one for computing the return and the other for capturing
 072 policy deviations. This decomposition isolates the impact of deviations, enabling a clearer and more
 073 accurate learning process. The conservative degree of each agent is dynamically adjusted based
 074 on the effect of their deviations on the overall return, promoting a balanced influence on system
 075 performance. This dynamic allocation is integrated into the OMCDA framework, ensuring a balance
 076 between conservatism and flexibility, and consistent credit assignment to enhance teamwork.

077 The key contributions of this paper are as follows: **(1)** A comprehensive analysis of conservative
 078 degree allocation in heterogeneous offline MARL, exploring how varying conservative degrees affect
 079 individual agent returns and overall system performance. **(2)** The introduction of OMCDA, a novel
 080 offline MARL algorithm that dynamically adjusts each agent’s conservative degree based on its
 081 impact on system performance, balancing conservatism and flexibility while ensuring consistent
 082 credit assignment and promoting collaboration. **(3)** Extensive experiments on diverse datasets,
 083 including multi-agent MuJoCo (de Witt et al., 2020) and the StarCraft Multi-Agent Challenge
 084 (SMAC) (Samvelyan et al., 2019), showing that OMCDA consistently outperforms existing methods
 085 across different environments and datasets.

086 2 PRELIMINARIES

087 We consider a MARL problem following (Wang et al., 2024) where the environment is modeled as a
 088 multi-agent Partially Observable Markov Decision Process (Boutilier, 1996), defined by the tuple:
 089 $G = \langle \mathcal{S}, \mathcal{A}, P, r, \mathcal{Z}, \mathcal{O}, n, \gamma \rangle$. $s \in \mathcal{S}$ is the true state of the environment. \mathcal{A} denotes the action set
 090 for each of the n agents. At every time step, each agent $i \in \{1, 2, \dots, n\}$ chooses an action $a_i \in \mathcal{A}$,
 091 forming a joint action $\mathbf{a} = (a_1, a_2, \dots, a_n) \in \mathcal{A}^n$. It causes a transition to the next state s' in the
 092 environment according to the transition dynamics $P(s'|s, \mathbf{a}) : \mathcal{S} \times \mathcal{A}^n \times \mathcal{S} \rightarrow [0, 1]$. All agents
 093 share the same global reward function $r(s, \mathbf{a}) : \mathcal{S} \times \mathcal{A}^n \rightarrow \mathbb{R}$. $\gamma \in [0, 1]$ is a discount factor. In
 094 the partially observable environment, each agent draws an observation $o_i \in \mathcal{O}$ at each step from the
 095 observation function $\mathcal{Z}(s, i) : \mathcal{S} \times N \rightarrow \mathcal{O}$. The objective of the team is to learn a set of policies
 096 $\pi = (\pi_1, \pi_2, \dots, \pi_n)$ that collectively maximize the expected discounted cumulative reward of the
 097 entire system. In the offline setting, agents do not interact with the environment directly but instead
 098 learn policies from a static dataset \mathcal{D} containing state-action-reward tuples. The challenge lies in
 099 learning effective policies without additional environment interactions.
 100

102 **CTDE Framework** The Centralized Training with Decentralized Execution (CTDE) framework is
 103 widely used in cooperative multi-agent reinforcement learning (MARL) (Oliehoek et al., 2008). In
 104 CTDE, agents are trained centrally with global information, enabling coordinated policy learning
 105 (Lowe et al., 2017). During execution, they act based on decentralized local observations, ensuring
 106 scalability in real-world settings. A key approach in this framework is value decomposition
 107 (Rashid et al., 2020; Sunehag et al., 2017; Wang et al., 2020a), where the global value function is
 factorized into local components for each agent. Algorithms such as QMIX (Rashid et al., 2020)

108 and VDN (Sunehag et al., 2017) employ monotonic value decomposition for scalable multi-agent
 109 learning. This framework has been adopted in offline MARL (Pan et al., 2022; Yang et al., 2021),
 110 with the global-local Q-value relationship:

$$112 \quad Q_{tot}(\mathbf{o}, \mathbf{a}) = \sum_i w_i(\mathbf{o}) Q_i(o_i, a_i) + b(\mathbf{o}), w_i \geq 0, \quad \forall i = 1 \dots n. \quad (1)$$

114 where $w_i(\mathbf{o})$, $b(\mathbf{o})$ are local function weights/bias and a_i , o_i are agent actions/observations.
 115

116 **Offline MARL with Policy regularization** Policy regularization constrains policy learning to
 117 remain close to the behavior policy (Xu et al., 2023), preventing out-of-distribution actions that
 118 could degrade performance. Several offline RL algorithms (Wu et al., 2019; Xu et al., 2023) use this
 119 approach to mitigate distributional shift. For example, BRAC (Wu et al., 2019) regularizes the actor’s
 120 policy to stay close to the behavior policy while optimizing the critic with the standard value function
 121 update. In offline MARL settings, this regularized method can be extended, with the objective written
 122 as:

$$123 \quad \max_{\pi} E \left[\sum_{t=0}^{\infty} \gamma^t r_t \right], \text{ s.t. } E_{a \sim \pi} [f(\pi(a_t | o_t), \pi_b(a_t | o_t))] \leq \epsilon. \quad (2)$$

124 Here $\pi = (\pi_1, \dots, \pi_N)$, f is a divergence term that quantifies how far the policy deviates from
 125 the behavior policy π_b , a_t and o_t are the action and state at timestep t , while ϵ is the constraint of
 126 f . We then convert the constrained optimization problem above into an unconstrained one using a
 127 Lagrangian relaxation by introducing a penalty hyperparameter α :

$$128 \quad \max_{\pi} \mathbb{E} \left[\sum_{t=0}^{\infty} \gamma^t (r_t - \alpha \cdot f(\pi(a_t | o_t), \pi_b(a_t | o_t))) \right]. \quad (3)$$

131 In this paper, we use Kullback-Leibler (KL) divergence (Pérez-Cruz, 2008) expressed as D_{KL} to
 132 constrain the learning policy and behaviour policy, while the Q-function can be formulated as:
 133

$$134 \quad Q(o, a) = \mathbb{E} \left[\sum_{t=0}^{\infty} \gamma^t (r_t - \alpha \cdot D_{KL}(\pi_t \| \pi_b)) \right], \quad (4)$$

137 where π_t and r_t are the policy and reward at timestep t . To address the issue of conservative degree
 138 allocation, we provide different levels of conservatism to agents in offline MARL by assigning each
 139 agent i an individual **conservative degree** d_i , which defines the permissible range of deviation from
 140 its behavior policy. The problem is then reformulated as the following:

$$141 \quad \max_{\pi} E \left[\sum_{t=0}^{\infty} \gamma^t r_t \right], \quad \text{s.t. } E_{a \sim \pi} \left[\log \frac{\pi_t^i(a_t^i | o_t^i)}{\pi_b(a_t^i | o_t^i)} \right] \leq d_i, \quad \sum_i d_i = d_{tot}, \quad \forall i = 1 \dots n. \quad (5)$$

143 Where d_i is the local conservative degree, and d_{tot} is the global conservative degree which is a fixed
 144 value. A deeper analysis of Eq. (5), which reveals the origin of the deviation term in Eq. (12), is
 145 provided in Appendix E.5. Then similar to the process of transitioning from Eq. (2) to Eq. (3), we
 146 can convert Eq. (5) and assign a **conservatism level** to each agent i , denoted as α_i , while the current
 147 Q-function can be formulated as:

$$148 \quad Q(o, a) = \mathbb{E} \left[\sum_{t=0}^{\infty} \gamma^t \left(r_t - \sum_i \alpha_i \cdot D_{KL}(\pi_t^i \| \pi_b) \right) \right]. \quad (6)$$

151 In the next section, OMCDA is introduced, built upon the decomposition of the Q-function and
 152 dynamic conservative degree allocation. We will demonstrate how this framework addresses the
 153 challenges of conservative degree allocation and emphasize its advantages in offline MARL systems.
 154

155 3 OMCDA

158 In this section, we present OMCDA for dynamic conservative degree allocation in offline MARL.
 159 First, we motivate the problem through a simple example, then decompose the Q-function to quantify
 160 individual agent contributions. We develop an adaptive mechanism that adjusts each agent’s conser-
 161 vatism according to its impact on system rewards. OMCDA ensures conservatism levels align with
 agents’ influence on returns, enhancing performance while preserving consistent credit assignment.

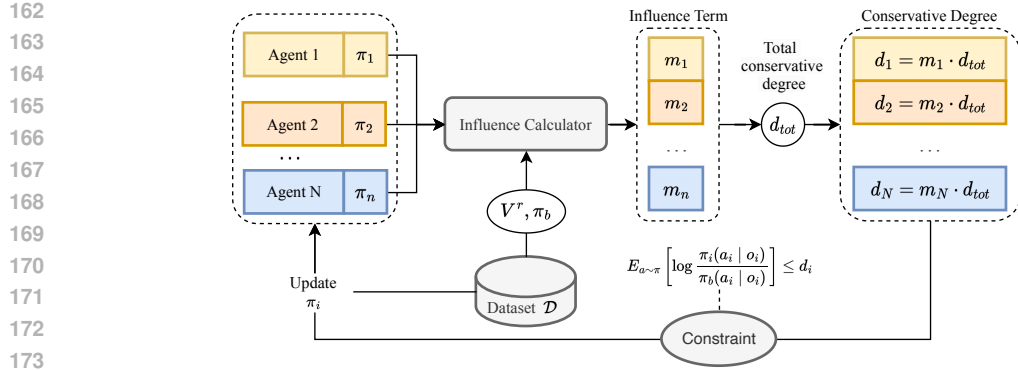


Figure 1: Overview of dynamic conservative degree allocation framework in OMCDA. 1) The influence calculator takes the policy from each agent, along with the return-based state-value function V^r and the behavior policy π_b derived from the data in dataset, as input to generate the influence term for each agent on the system. 2) Each agent’s conservative degree is then allocated from the total conservative degree based on the influence term. 3) Finally, the conservative degree is integrated as a network update constraint, enabling dynamic allocation while ensuring consistent credit assignment.

Conservative Degree Allocation in Offline MARL In offline MARL, agents’ influences on the system are not uniform. To fully leverage these influences and improve system performance, dynamic conservative degree allocation is necessary. This approach allows high-impact agents to make larger deviations, enhancing their contribution to the overall performance. To better illustrate this issue, we present a 2-player toy example in Table 1.

In this game, we employ a **mixed strategy**. As a cooperative team, individual players cannot access their personal rewards directly; instead, they observe the team’s expected reward r_{team} which is :

$$\sum_{a_1 \in \{A, B\}} \sum_{a_2 \in \{A, B\}} \pi_1(a_1) \pi_2(a_2) r(a_1, a_2). \quad (7)$$

The game features two possible actions (A and B) for each player. Consider both players following a uniform behavior policy $\pi_b = (0.5, 0.5)$. The offline dataset \mathcal{D} is collected under π_b , containing policy pairs with their corresponding team reward r_{team} : $\mathcal{D} = \{(\pi_1 = (0.5, 0.5), \pi_2 = (0.5, 0.5), r_{team})\}$. Clearly, Player 1 achieves higher rewards and greater influence on team performance than Player 2, justifying greater allowance for policy deviation. We quantify deviation of agent i ’s policy from behavior policy through Manhattan distance (Chiu et al., 2016) $\Delta_i = \sum_{a \in \{A, B\}} |\pi_i(a) - \pi_{behavior}(a)|$.

To align with traditional offline methods, the total conservative degree Δ_{total} for the entire system is set to 0.4. Under uniform conservative allocation, both players share the total deviation equally: $\Delta_1 = \Delta_2 = 0.2$. After training, the optimal strategies for both players are $(0.6, 0.4)$, increasing team’s expected reward by 0.1. Under dynamic allocation, Player 1 receives a larger deviation: $\Delta_1 = 0.3$, reflecting its higher impact, while $\Delta_2 = 0.1$. Consequently, Player 1 learns a more aggressive strategy $(0.65, 0.35)$, while Player 2 remains near the behavior policy $(0.55, 0.45)$. The dynamic allocation improves team’s expected reward more by 0.15, demonstrating its effectiveness in coordinating heterogeneous agents.

Decomposition Framework We now present the decomposition framework for value functions, aiming to assign different conservative degrees to each agent, as described in Eq. (5). To achieve this, it’s crucial to understand how an agent’s deviation from the behavior policy affects the overall return. In offline RL with regularization, both the Q-function and value function contain entangled return and constraint components (Eq. 4), complicating the measurement of an agent’s influence on

the return. Inspired by BOPAH (Lee et al., 2020), our framework disentangles these components by decomposing the Q-function and value function into two parts: one that computes the return and another that accounts for the deviation constraint. In our framework, the original Q-function in offline RL with regularization in Eq.(4) can be written as:

$$Q(o, a) = Q^r(o, a) + \alpha \cdot Q^c(o, a), \quad Q^r := \mathbb{E} \left[\sum_{t=0}^{\infty} \gamma^t r_t \right], \quad Q^c := \mathbb{E} \left[- \sum_{t=1}^{\infty} \gamma^t D_{\text{KL}}(\pi_t \parallel \pi_b) \right]. \quad (8)$$

In this definition, $Q^r(o, a)$ calculates the return, and $Q^c(o, a)$ captures the deviation from the behavior policy. Similar to these two Q-functions, the decomposition of V-function can also be obtained as:

$$V(o, a) = V^r(o, a) + \alpha \cdot V^c(o, a). \quad (9)$$

Then with the current Q-function and V-function, the corresponding Bellman backup operators is formulated as:

$$(\mathcal{T}_f^{\pi}) Q^r(o, a) := r(o, a) + \gamma \mathbb{E}_{o' \mid o, a} [V^r(o')], \quad (\mathcal{T}_f^{\pi}) Q^c(o, a) := \gamma \mathbb{E}_{o' \mid o, a} [V^c(o')], \quad (10)$$

where V-functions is written similar to SAC (Haarnoja et al., 2018) as:

$$V^r(o) = \mathbb{E}_{a \sim \pi} [Q^r(o, a)], \quad V^c(o) = \mathbb{E}_{a \sim \pi} \left[Q^c(o, a) - \log \left(\frac{\pi(a \mid o)}{\pi_b(a \mid o)} \right) \right]. \quad (11)$$

By decoupling the Q-function into separate return and deviation components, we isolate return calculation from conservatism enforcement. This enables precise assessment of each agent's influence on cumulative returns, free from conservatism constraint interference. This approach proves particularly crucial in offline MARL, where individual actions affect the joint return. When extending to multi-agent case, according to Eq. (6) and the definitions in Eq. (8), the global Q-function (a detailed analysis of the relationship between Eq. (5) and the deviation term in Eq. (12) is provided in Appendix E.5) can be derived within the QMIX framework (Rashid et al., 2020) as follows:

$$Q_{\text{tot}}(o, a) = Q_{\text{tot}}^r(o, a) + \sum_{i=1}^N \alpha_i \cdot Q^{c,i}(o, a), \quad (12)$$

where

$$Q_{\text{tot}}^r(o, a) = \sum_i w_i^r(o) Q_i^r(o_i, a_i) + b^r(o), \quad (13)$$

$$Q^{c,i}(o, a) = \sum_j w_j^{c,i}(o) Q_j^c(o_j, a_j) + b^{c,i}(o). \quad (14)$$

In Eq. (13), Q_{tot}^r represents the global return information, which is distributed to individual agents through value decomposition, with w^r and b^r as the weight and bias parameters for each agent's local return function Q_i^r . Eq. (14) defines agent i 's conservatism value function $Q^{c,i}(o, a)$, computed as a weighted sum over all agents' conservatism values $Q_j^c(o_j, a_j)$. Here, $w_j^{c,i}(o)$ denotes the observation-dependent weight for agent j 's contribution to agent i 's conservatism, while $b^{c,i}(o)$ serves as an adaptive bias term. The decomposition of the V-function is derived in the same manner as the Q-function. The decomposed forms of V_{tot}^r and $V^{c,i}$ are expressed as follows:

$$V_{\text{tot}}^r(o) = \sum_i w_i^r(o) V_i^r(o_i) + b^r(o), \quad (15)$$

$$V^{c,i}(o) = \sum_j w_j^{c,i}(o) V_j^c(o_j) + b^{c,i}(o). \quad (16)$$

With the decomposition framework, each agent can balance both individual and global constraints effectively, while also more accurately assessing both its own and the overall system's return.

270 **Dynamic Conservative Degree Allocation for Agents in Offline MARL Setting** After we get our
 271 decomposition framework, since the goal to maximum the return is equal to maximum global return-
 272 based state-value function V_{tot}^r . The maximum term in Eq.(5) can be changed into $\max_{\pi} \mathbb{E} [V_{tot}^r(o)]$.
 273

274 Next, we illustrate the approach to develop a dynamic adaptation method (shown in Figure. 1) that
 275 adjusts the conservative degrees for agents dynamically. Let us take another look at the constraint
 276 term in Eq.(5) where we want to adaptively assign a conservative degree d_i to each agent. Given
 277 the total degree d_{tot} , an efficient strategy is to allocate it based on the influence of the agents on the
 278 system. Hence, we propose an influence term \mathbf{m}_i for each agent i , and d_i can be obtained as:
 279

$$d_i = \mathbf{m}_i \cdot d_{tot}. \quad (17)$$

280 As shown in Table 1, in offline MARL settings, an agent's influence on the system determines the
 281 sensitivity of the system to its behavioral policy deviations. Thus, we quantify each agent's influence
 282 as the impact of its policy deviation on the collective return V_{tot}^r . Taking the expression of V_{tot}^r
 283 in Eq.(11) into account, the influence can be derived by computing the partial derivative of the
 284 return-based value function V_{tot}^r with respect to the KL divergence between the agent's current policy
 285 π_i and its own behavior policy π_b^i following:
 286

$$\mathbf{m}_i = \frac{\partial V_{tot}^r(o)}{\partial D_{KL}(\pi_i \parallel \pi_b^i)}. \quad (18)$$

290 In practice, to facilitate computation, the chain rule is applied to break down complex dependencies
 291 between $V_{tot}^r(o)$ and the KL divergence $D_{KL}(\pi^i \parallel \pi_b^i)$, enabling efficient influence computation
 292 (further details are in Appendix E.2):
 293

$$\mathbf{m}_i = \frac{\partial V_{tot}^r(o)}{\partial \pi_i} \left(\frac{\partial D_{KL}(\pi_i \parallel \pi_b^i)}{\partial \pi_i} \right)^{-1}. \quad (19)$$

297 The first term in Eq.(19) captures the strategy change's system impact, while the second term acts
 298 as a constraint, measuring the agent's deviation from its behavior policy. Since V_{tot}^r isolates the
 299 conservatism term from V_{tot} , it directly quantifies how policy deviations affect system returns.
 300 This reveals the relationship between an agent's policy deviation and its return impact. Eq.(18)
 301 dynamically determines each agent's conservatism constraint, measuring system return sensitivity
 302 to policy deviations. A larger derivative indicates greater positive return impact, permitting more
 303 flexible d_i ; smaller derivatives warrant stricter constraints to mitigate risk. Due to $\sum_i d_i = d_{tot}$
 304 in Eq.(5), to determine the appropriate conservative degree d_i for each agent, we adopt a softmax
 305 function to normalize the weights across all agents:
 306

$$\mathbf{m} = [\mathbf{m}_1, \dots, \mathbf{m}_N] = \text{Softmax} \left[\mathbb{E} \left[\frac{\partial V_{tot}^r(o)}{\partial D_{KL}(\pi_1 \parallel \pi_b^1)} \right], \dots, \mathbb{E} \left[\frac{\partial V_{tot}^r(o)}{\partial D_{KL}(\pi_N \parallel \pi_b^N)} \right] \right]. \quad (20)$$

309 After obtaining m_i , each d_i can be derived using Eq.(17). The conservatism level α_i introduced in
 310 Eq.(12) can be updated according to following objective:
 311

$$\min_{\alpha_i} (\alpha_i \cdot d_i - \alpha_i \cdot D_{KL}(\pi_i \parallel \pi_b^i)). \quad (21)$$

314 With the conservatism levels α_i obtained for each agent, we apply these dynamic adjustments to the
 315 offline MARL environment. We begin by deriving the optimal global policy in the offline MARL
 316 setting in Proposition 3.1.
 317

318 **Proposition 3.1.** *In an offline MARL setting, the optimal global policy $\pi_{tot}^*(a \mid o)$ is given by Eq. (4)
 319 and is formally expressed as follows:*

$$\pi_{tot}^*(a \mid o) = \pi_b(a \mid o) \cdot \exp \left(\frac{1}{\alpha} (Q^*(o, a) - V^*(o)) \right), \quad (22)$$

320 where $Q^*(o, a)$ is optimal action-value function, $V^*(o)$ is optimal value function, and a global
 321 conservatism level α is assumed that controls the overall deviation from the behavior policy.
 322

The proof is based on the principles of soft Q-learning(Haarnoja et al., 2018) and we extend it to offline MARL context. Then, we aim to derive the local optimal policy from the global optimal policy in Eq.(22) by applying the individual conservatism level α_i for each agent in Proposition 3.2, and demonstrate its validity in Theorem 3.3.

Proposition 3.2. *Joint policy π_{tot} is decomposed into product of individual agent policies π_i as:*

$$\pi_{tot}(a | o) = \prod_{i=1}^N \pi_i(a_i | o_i).$$

Based on decomposition in Eq.(12) - (16), the optimal policy $\pi_i^*(a_i | o_i)$ for each agent is given by:

$$\pi_i^*(a_i | o_i) = \pi_b(a_i | o_i) \cdot \exp \left(\frac{w_i^r(\mathbf{o})}{\alpha_i} \left(Q_i^{r*}(o_i, a_i) - V_i^{r*}(o_i) \right) + \left(Q^{c,i*}(\mathbf{o}, a) - V^{c,i*}(\mathbf{o}) \right) \right), \quad (23)$$

where α_i controls the conservatism level of the agent’s policy, and π_i^* denotes the **optimal policy** that satisfies Eq.(5).

Theorem 3.3. *Given Eq.(23), the optimal policy for each agent is derived, and consistency between the local optimal policies π_i^* and the global optimal policy π_{tot}^* is guaranteed. This consistency holds for individual α_i assignments across agents.*

The optimal π_i^* is then used to update each agent’s conservatism-based value function V_i^c . It should be noted that each local policy needs to satisfy $\sum_{a_i \sim \pi_i} \pi_i^*(a_i | o_i) = 1$. Therefore, according to Eq.(23), the following formula can be obtained:

$$\mathbb{E}_{a_i \sim \pi_b} \left[\exp \left(\frac{w_i^r(\mathbf{o})}{\alpha_i} \left(Q_i^{r*}(o_i, a_i) - V_i^{r*}(o_i) \right) + \left(Q^{c,i*}(\mathbf{o}, a) - V^{c,i*}(\mathbf{o}) \right) \right) \right] = 1. \quad (24)$$

Proposition 3.4. *From Eq.(24), each agent’s conservatism-based value function V_i^c is updated through the following optimization:*

$$\begin{aligned} \min_{V_i^c} \mathbb{E}_{(o_i, a_i) \sim \mathcal{D}} & \left[\exp \left(\frac{w_i^r(\mathbf{o})}{\alpha_i} (Q_i^r(o_i, a_i) - V_i^r(o_i)) \right. \right. \\ & \left. \left. + (Q^{c,i}(o, a) - V^{c,i}(o)) \right) + \frac{w_i^r(\mathbf{o}) V_i^r(o_i) + \alpha_i V^{c,i}(o)}{\alpha_i} \right]. \end{aligned} \quad (25)$$

The proofs of Proposition 3.1, Proposition 3.4 and Theorem 3.3 are provided in Appendix C.

Dynamic conservatism has now been incorporated into MARL frameworks, enabling agents to optimize their behavior in offline settings through adaptive balancing between conservatism and policy deviation—with each agent’s contribution weighted by its measured impact on collective system performance. The algorithm and additional explanation of OMCDA is in Appendix E.1.

Comparison with prior works Prior works including FOP (Zhang et al., 2021), ADER (Kim & Sung, 2023), and CFCQL (Shao et al., 2024) have investigated adaptive approaches in MARL. While FOP and ADER are online methods that employ dynamic entropy regularization similar to OMCDA, their adaptive mechanisms are confined to policy updates, applying either global uniform constraints or no constraints to Q/V function updates—an approach that fails to address per-agent constraint allocation for heterogeneous agents, which is crucial for mitigating OOD issues in offline MARL. In contrast, OMCDA uniquely enables dynamic conservatism allocation for both policies and value functions, ensuring optimal updates in offline settings. Offline method CFCQL determines conservatism by behavior policy deviation, while OMCDA considers each agent’s impact on system performance. This allows OMCDA to balance conservatism and flexibility, optimizing performance.

4 EXPERIMENT

In this section, we conduct experiments to: (1) evaluate OMCDA’s performance, (2) demonstrate its effectiveness in dynamic conservative degree allocation, and (3) analyze key components and choices of total conservative degrees. Further ablation details are in Appendix F.

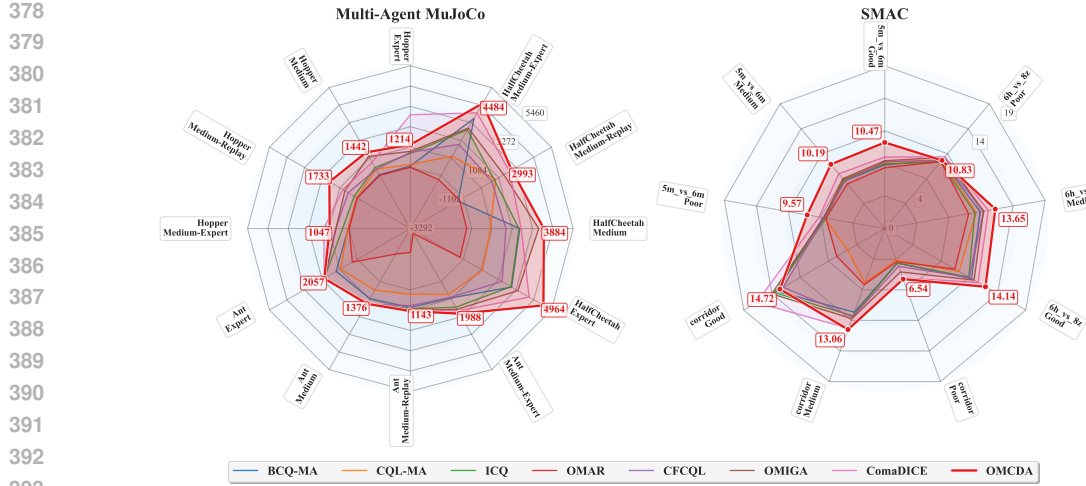


Figure 2: The average returns for the offline Multi-Agent MuJoCo and SMAC

Offline Multi-Agent Datasets We select **Multi-Agent MuJoCo**(de Witt et al., 2020) and the **StarCraft Multi-Agent Challenge (SMAC)**(Samvelyan et al., 2019) as our experiment environments. Multi-Agent MuJoCo, a benchmark for continuous multi-agent robotic control, is built on the MuJoCo environment. The Multi-Agent MuJoCo dataset we use was collected using the HAPPO(Kuba et al., 2021) algorithm by (Wang et al., 2024) which contains four quality levels: expert, medium, medium-replay and medium-expert. The second environment, SMAC, is a widely-used benchmark for evaluating cooperative MARL methods. The offline SMAC dataset is collected by (Meng et al., 2021), using online-trained MAPPO(Kuba et al., 2021) agents. This is the largest publicly available dataset for SMAC and includes three quality levels: good, medium, and poor. We focus on three representative battle maps in our experiments: one hard map (5m_vs_6m) and two super hard maps (6h_vs_8z and corridor). We initialize the **behavior policy** π_b through behavior cloning (Michie et al., 1990) using the offline dataset. Further details on these datasets are provided in Appendix D.

Baselines and Comparative Evaluation We compare our approach with seven offline MARL algorithms: The multi-agent versions of BCQ(Fujimoto et al., 2019) and CQL(Kostrikov et al., 2021b) (referred to as BCQ-MA and CQL-MA), ICQ(Yang et al., 2021), OMAR(Pan et al., 2022), CFCQL(Shao et al., 2024), OMIGA(Wang et al., 2024), and ComaDICE(Bui et al., 2024). Both BCQ-MA and CQL-MA utilize a linear weighted value decomposition for the multi-agent setting, similar to Eq. (1). Hyperparameters used in our experiments are provided in Appendix E.4. Figure 2 presents returns for the offline Multi-Agent MuJoCo and SMAC tasks with 5 random seeds. Detailed analysis of the results and the mean and standard deviation of returns are in Appendix E.3.

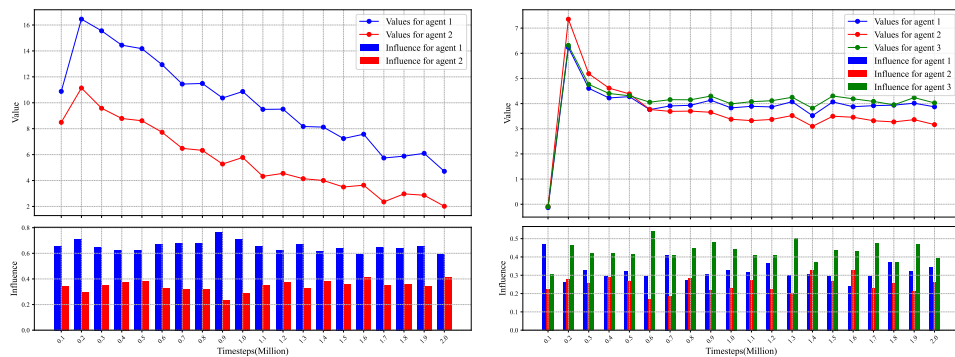
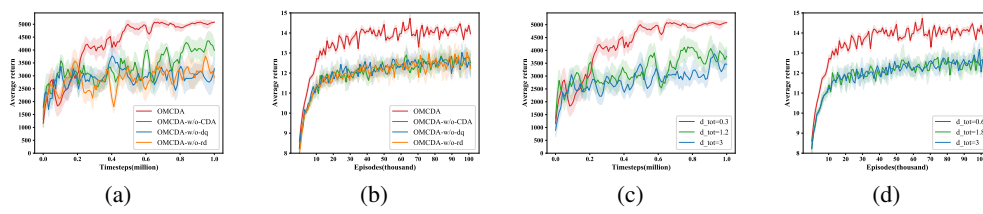


Figure 3: Analysis on the influence term on Ant(left) and Hopper(right)

432 **Analysis on the Influence Term** In OMCDA, the influence of each agent on the system is the
 433 core metric for allocating conservatism levels. We conduct experiments to analyze the relationship
 434 between the computed influence of each agent and its corresponding return. The results in Figure. 3
 435 demonstrate that agents with higher V_i^r , representing higher individual returns, tend to be allocated
 436 more influence, enabling them to have a stronger impact on system performance. This proportional
 437 allocation allows high-return agents to further contribute to global objectives and optimize overall
 438 behaviour. By adjusting conservatism levels properly, OMCDA enhances individual performance and
 439 maximizes collective return, promoting balanced and efficient learning across agents.

440 **Analysis on the Components of OMCDA** To analyze conservative degree allocation and the im-
 441 pact of Q-function decomposition in OMCDA, we conduct three ablation studies: OMCDA-w/o-CDA,
 442 OMCDA-w/o-dq, and OMCDA-rd. In OMCDA-w/o-CDA, all agents share the same conservative
 443 degree d_i without allocation. In OMCDA-w/o-dq, dynamic allocation remains but Q-function decom-
 444 position is removed, entangling return optimization with deviation handling. OMCDA-rd assigns each
 445 agent a random d_i , used to evaluate the role of strategic assignment. Experiments on HalfCheetah and
 446 6h_vs_8z in the Multi-agent MuJoCo and SMAC environments show that OMCDA consistently out-
 447 performs all ablated versions (Figure. 4a-b). Lacking dynamic allocation, OMCDA-w/o-CDA causes
 448 imbalance and degraded performance. OMCDA-w/o-dq weakens learning as objectives become
 449 entangled, while OMCDA-rd performs worse since random d_i ignores agents' distinct impact. These
 450 results confirm that dynamic allocation and Q-function decomposition are essential for collaboration
 451 and efficiency in offline multi-agent environments, while strategic assignment of conservatism is
 452 crucial for optimal system performance.



453
 454
 455 Figure 4: Analyses and ablations of OMCDA. We analyze the effect of model components **(a-b)** and
 456 total conservative degree **(c-d)** across HalfCheetah from MA-MuJoCo and 6h_vs_8z from SMAC.
 457
 458

462 **Analysis on the Total Conservative Degree** The total conservative degree d_{tot} controls how much
 463 the system may deviate from the behavior policy. It sets the permissible deviation for the entire system,
 464 ensuring agents do not diverge excessively. In experiments on HalfCheetah and 6h_vs_8z, based on
 465 high-quality datasets, a smaller d_{tot} outperforms other settings. This is because in such environments
 466 it is essential for policies to stay closer to the behavior policy for stable performance. Meanwhile,
 467 dynamic allocation of d_i allows agents with significant impact on returns some flexibility to deviate,
 468 while requiring others to remain conservative and adhere closely to the behavior policy. The results
 469 in Figure. 4(c-d) show that adjusting d_{tot} improves overall performance, allowing influential agents
 470 beneficial deviations while maintaining system stability.

475 5 CONCLUSION

478 In conclusion, a novel offline MARL framework OMCDA is introduced to tackle the challenge
 479 of conservative degree allocation. OMCDA decomposes the Q-function in offline MARL with
 480 regularization into two components: one for computing the return and another for capturing deviations
 481 from the behavior policy. It dynamically adjusts each agent's conservative degree based on their
 482 influence on the overall system's performance, ensuring coherent credit assignment and robust
 483 performance throughout the learning process. Meanwhile, extensive experiments demonstrate that
 484 OMCDA consistently outperforms existing offline MARL methods across various environments. Our
 485 future works aim to enhance OMCDA by developing adaptive mechanisms that reduce sensitivity to
 486 total conservative degree selection, and lower the computational complexity.

486 REFERENCES
487

488 Chenjia Bai, Lingxiao Wang, Zhuoran Yang, Zhihong Deng, Animesh Garg, Peng Liu, and Zhaoran
489 Wang. Pessimistic bootstrapping for uncertainty-driven offline reinforcement learning. *arXiv*
490 *preprint arXiv:2202.11566*, 2022.

491 Christopher Berner, Greg Brockman, Brooke Chan, Vicki Cheung, Przemysław Dębiak, Christy
492 Dennison, David Farhi, Quirin Fischer, Shariq Hashme, Chris Hesse, et al. Dota 2 with large scale
493 deep reinforcement learning. *arXiv preprint arXiv:1912.06680*, 2019.

494 Craig Boutilier. Planning, learning and coordination in multiagent decision processes. In *TARK*,
495 volume 96, pp. 195–210. Citeseer, 1996.

496 David Brandfonbrener, Will Whitney, Rajesh Ranganath, and Joan Bruna. Offline rl without off-policy
497 evaluation. *Advances in neural information processing systems*, 34:4933–4946, 2021.

498 The Viet Bui, Thanh Hong Nguyen, and Tien Mai. Comadice: Offline cooperative multi-agent
499 reinforcement learning with stationary distribution shift regularization, 2024. URL <https://arxiv.org/abs/2410.01954>.

500 Yongcan Cao, Wenwu Yu, Wei Ren, and Guanrong Chen. An overview of recent progress in the
501 study of distributed multi-agent coordination. *IEEE Transactions on Industrial informatics*, 9(1):
502 427–438, 2012.

503 Peng Cheng, Xianyuan Zhan, Wenjia Zhang, Youfang Lin, Han Wang, Li Jiang, et al. Look beneath
504 the surface: Exploiting fundamental symmetry for sample-efficient offline rl. *Advances in Neural*
505 *Information Processing Systems*, 36, 2024.

506 Wei-Yu Chiu, Gary G Yen, and Teng-Kuei Juan. Minimum manhattan distance approach to mul-
507 tiple criteria decision making in multiobjective optimization problems. *IEEE Transactions on*
508 *Evolutionary Computation*, 20(6):972–985, 2016.

509 Christian Schroeder de Witt, Bei Peng, Pierre-Alexandre Kamienny, Philip Torr, Wendelin Böhmer,
510 and Shimon Whiteson. Deep multi-agent reinforcement learning for decentralized continuous
511 cooperative control. *arXiv preprint arXiv:2003.06709*, 19, 2020.

512 Jakob Foerster, Gregory Farquhar, Triantafyllos Afouras, Nantas Nardelli, and Shimon Whiteson.
513 Counterfactual multi-agent policy gradients. In *Proceedings of the AAAI conference on artificial*
514 *intelligence*, volume 32, 2018.

515 Scott Fujimoto and Shixiang Shane Gu. A minimalist approach to offline reinforcement learning.
516 *Advances in neural information processing systems*, 34:20132–20145, 2021.

517 Scott Fujimoto, David Meger, and Doina Precup. Off-policy deep reinforcement learning without
518 exploration. In *International conference on machine learning*, pp. 2052–2062. PMLR, 2019.

519 Tuomas Haarnoja, Aurick Zhou, Pieter Abbeel, and Sergey Levine. Soft actor-critic: Off-policy
520 maximum entropy deep reinforcement learning with a stochastic actor. In *International conference*
521 *on machine learning*, pp. 1861–1870. PMLR, 2018.

522 Pablo Hernandez-Leal, Bilal Kartal, and Matthew E Taylor. A survey and critique of multiagent deep
523 reinforcement learning. *Autonomous Agents and Multi-Agent Systems*, 33(6):750–797, 2019.

524 Jiechuan Jiang and Zongqing Lu. Offline decentralized multi-agent reinforcement learning. In *ECAI*,
525 pp. 1148–1155, 2023.

526 Woojun Kim and Youngchul Sung. An adaptive entropy-regularization framework for multi-agent
527 reinforcement learning. In *International Conference on Machine Learning*, pp. 16829–16852.
528 PMLR, 2023.

529 Ilya Kostrikov, Rob Fergus, Jonathan Tompson, and Ofir Nachum. Offline reinforcement learning
530 with fisher divergence critic regularization. In *International Conference on Machine Learning*, pp.
531 5774–5783. PMLR, 2021a.

540 Ilya Kostrikov, Ashvin Nair, and Sergey Levine. Offline reinforcement learning with implicit
 541 q-learning. *arXiv preprint arXiv:2110.06169*, 2021b.
 542

543 Landon Kraemer and Bikramjit Banerjee. Multi-agent reinforcement learning as a rehearsal for
 544 decentralized planning. *Neurocomputing*, 190:82–94, 2016.
 545

546 Jakub Grudzien Kuba, Ruiqing Chen, Muning Wen, Ying Wen, Fanglei Sun, Jun Wang, and Yaodong
 547 Yang. Trust region policy optimisation in multi-agent reinforcement learning. *arXiv preprint
 548 arXiv:2109.11251*, 2021.
 549

549 Aviral Kumar, Justin Fu, Matthew Soh, George Tucker, and Sergey Levine. Stabilizing off-policy
 550 q-learning via bootstrapping error reduction. *Advances in neural information processing systems*,
 551 32, 2019.
 552

552 Aviral Kumar, Aurick Zhou, George Tucker, and Sergey Levine. Conservative q-learning for offline
 553 reinforcement learning. *Advances in Neural Information Processing Systems*, 33:1179–1191, 2020.
 554

555 Byungjun Lee, Jongmin Lee, Peter Vrancx, Dongho Kim, and Kee-Eung Kim. Batch reinforcement
 556 learning with hyperparameter gradients. In *International Conference on Machine Learning*, pp.
 557 5725–5735. PMLR, 2020.
 558

558 Sergey Levine, Aviral Kumar, George Tucker, and Justin Fu. Offline reinforcement learning: Tutorial,
 559 review, and perspectives on open problems. *arXiv preprint arXiv:2005.01643*, 2020.
 560

561 Zongkai Liu, Qian Lin, Chao Yu, Xiawei Wu, Yile Liang, Donghui Li, and Xuetao Ding. Offline
 562 multi-agent reinforcement learning via in-sample sequential policy optimization, 2024. URL
 563 <https://arxiv.org/abs/2412.07639>.
 564

564 Ryan Lowe, Yi I Wu, Aviv Tamar, Jean Harb, OpenAI Pieter Abbeel, and Igor Mordatch. Multi-agent
 565 actor-critic for mixed cooperative-competitive environments. *Advances in neural information
 566 processing systems*, 30, 2017.
 567

568 Daiki E. Matsunaga, Jongmin Lee, Jaeseok Yoon, Stefanos Leonardos, Pieter Abbeel, and Kee-Eung
 569 Kim. Alberdice: Addressing out-of-distribution joint actions in offline multi-agent rl via alternating
 570 stationary distribution correction estimation, 2023. URL <https://arxiv.org/abs/2311.02194>.
 571

572 Linghui Meng, Muning Wen, Yaodong Yang, Chenyang Le, Xiyun Li, Weinan Zhang, Ying Wen,
 573 Haifeng Zhang, Jun Wang, and Bo Xu. Offline pre-trained multi-agent decision transformer: One
 574 big sequence model tackles all smac tasks. *arXiv preprint arXiv:2112.02845*, 2021.
 575

576 Donald Michie, Michael Bain, and J Hayes-Miches. Cognitive models from subcognitive skills. *IEE
 577 control engineering series, IEE control engineering series*, Jan 1990.
 578

578 Frans A Oliehoek, Matthijs TJ Spaan, and Nikos Vlassis. Optimal and approximate q-value functions
 579 for decentralized pomdps. *Journal of Artificial Intelligence Research*, 32:289–353, 2008.
 580

581 James Orr and Ayan Dutta. Multi-agent deep reinforcement learning for multi-robot applications: A
 582 survey. *Sensors*, 23(7):3625, 2023.
 583

583 Ling Pan, Longbo Huang, Tengyu Ma, and Huazhe Xu. Plan better amid conservatism: Offline
 584 multi-agent reinforcement learning with actor rectification. In *International conference on machine
 585 learning*, pp. 17221–17237. PMLR, 2022.
 586

587 Xue Bin Peng, Aviral Kumar, Grace Zhang, and Sergey Levine. Advantage-weighted regression:
 588 Simple and scalable off-policy reinforcement learning. *arXiv preprint arXiv:1910.00177*, 2019.
 589

590 Fernando Pérez-Cruz. Kullback-leibler divergence estimation of continuous distributions. In *2008
 591 IEEE international symposium on information theory*, pp. 1666–1670. IEEE, 2008.
 592

592 Tabish Rashid, Mikayel Samvelyan, Christian Schroeder De Witt, Gregory Farquhar, Jakob Foerster,
 593 and Shimon Whiteson. Monotonic value function factorisation for deep multi-agent reinforcement
 594 learning. *Journal of Machine Learning Research*, 21(178):1–51, 2020.

594 Mikayel Samvelyan, Tabish Rashid, Christian Schroeder De Witt, Gregory Farquhar, Nantas Nardelli,
 595 Tim GJ Rudner, Chia-Man Hung, Philip HS Torr, Jakob Foerster, and Shimon Whiteson. The
 596 starcraft multi-agent challenge. *arXiv preprint arXiv:1902.04043*, 2019.

597

598 Jianzhen Shao, Yun Qu, Chen Chen, Hongchang Zhang, and Xiangyang Ji. Counterfactual conservative
 599 q learning for offline multi-agent reinforcement learning. *Advances in Neural Information
 600 Processing Systems*, 36, 2024.

601 Peter Sunehag, Guy Lever, Audrunas Gruslys, Wojciech Marian Czarnecki, Vinicius Zambaldi, Max
 602 Jaderberg, Marc Lanctot, Nicolas Sonnerat, Joel Z Leibo, Karl Tuyls, et al. Value-decomposition
 603 networks for cooperative multi-agent learning. *arXiv preprint arXiv:1706.05296*, 2017.

604

605 Jianhao Wang, Zhizhou Ren, Terry Liu, Yang Yu, and Chongjie Zhang. Qplex: Duplex dueling
 606 multi-agent q-learning. *arXiv preprint arXiv:2008.01062*, 2020a.

607 Tonghan Wang, Heng Dong, Victor Lesser, and Chongjie Zhang. Roma: Multi-agent reinforcement
 608 learning with emergent roles. *arXiv preprint arXiv:2003.08039*, 2020b.

609

610 Xiangsen Wang and Xianyuan Zhan. Offline multi-agent reinforcement learning with coupled value
 611 factorization. *arXiv preprint arXiv:2306.08900*, 2023.

612

613 Xiangsen Wang, Haoran Xu, Yinan Zheng, and Xianyuan Zhan. Offline multi-agent reinforcement
 614 learning with implicit global-to-local value regularization. *Advances in Neural Information
 615 Processing Systems*, 36, 2024.

616

617 Ziyang Wang, Yali Du, Yudi Zhang, Meng Fang, and Biwei Huang. Macca: Offline multi-agent
 618 reinforcement learning with causal credit assignment. *arXiv preprint arXiv:2312.03644*, 2023.

619

620 Yifan Wu, George Tucker, and Ofir Nachum. Behavior regularized offline reinforcement learning.
 621 *arXiv preprint arXiv:1911.11361*, 2019.

622

623 Yue Wu, Shuangfei Zhai, Nitish Srivastava, Joshua Susskind, Jian Zhang, Ruslan Salakhutdinov, and
 624 Hanlin Goh. Uncertainty weighted actor-critic for offline reinforcement learning. *arXiv preprint
 625 arXiv:2105.08140*, 2021.

626

627 Haoran Xu, Xianyuan Zhan, Jianxiong Li, and Honglei Yin. Offline reinforcement learning with soft
 628 behavior regularization. *arXiv preprint arXiv:2110.07395*, 2021.

629

630 Haoran Xu, Li Jiang, Jianxiong Li, Zhuoran Yang, Zhaoran Wang, Victor Wai Kin Chan, and
 631 Xianyuan Zhan. Offline rl with no ood actions: In-sample learning via implicit value regularization.
 632 *arXiv preprint arXiv:2303.15810*, 2023.

633

634 Yiqin Yang, Xiaoteng Ma, Chenghao Li, Zewu Zheng, Qiyuan Zhang, Gao Huang, Jun Yang, and
 635 Qianchuan Zhao. Believe what you see: Implicit constraint approach for offline multi-agent
 636 reinforcement learning. *Advances in Neural Information Processing Systems*, 34:10299–10312,
 637 2021.

638

639 Tianhe Yu, Garrett Thomas, Lantao Yu, Stefano Ermon, James Y Zou, Sergey Levine, Chelsea Finn,
 640 and Tengyu Ma. Mopo: Model-based offline policy optimization. *Advances in Neural Information
 641 Processing Systems*, 33:14129–14142, 2020.

642

643 Xianyuan Zhan, Xiangyu Zhu, and Haoran Xu. Model-based offline planning with trajectory pruning.
 644 *arXiv preprint arXiv:2105.07351*, 2021.

645

646 Tianhao Zhang, Yueheng Li, Chen Wang, Guangming Xie, and Zongqing Lu. Fop: Factorizing
 647 optimal joint policy of maximum-entropy multi-agent reinforcement learning. In *International
 648 conference on machine learning*, pp. 12491–12500. PMLR, 2021.

649

650 Zhengbang Zhu, Minghuan Liu, Liyuan Mao, Bingyi Kang, Minkai Xu, Yong Yu, Stefano Ermon,
 651 and Weinan Zhang. Madiff: Offline multi-agent learning with diffusion models, 2025. URL
 652 <https://arxiv.org/abs/2305.17330>.

653

654

648 **A USE OF LARGE LANGUAGE MODELS (LLMs)**
649650 We employed the large language model as an auxiliary tool during manuscript preparation. Specif-
651 ically, it was used to refine language for grammar and clarity, and to generate illustrative (non-
652 experimental) figures based on prompts we provided. All research ideas, methods, experiments,
653 analyses, and conclusions were developed by the authors.
654655 **B RELATED WORK**
656657 **B.1 OFFLINE REINFORCEMENT LEARNING**
658659 Offline reinforcement learning must address distributional shift (Kumar et al., 2019), which occurs
660 when policies encounter out-of-distribution (OOD) states or actions (Fujimoto et al., 2019), leading
661 to exploitation errors and poor performance due to inaccurate value estimates on OOD actions.
662663 To mitigate this, policy constraint methods (Cheng et al., 2024; Fujimoto et al., 2019; Xu et al., 2021)
664 aim to keep the learned policy close to the behavior policy, reducing deviations from the training
665 data. Value regularization techniques (Kostrikov et al., 2021a) (Kumar et al., 2020) penalize OOD
666 value estimates, while uncertainty-based (Bai et al., 2022; Wu et al., 2021) and model-based (Yu
667 et al., 2020; Zhan et al., 2021) approaches focus on penalizing actions in uncertain or sparse regions.
668 Recently, in-sample learning methods (Brandfonbrener et al., 2021; Kostrikov et al., 2021b; Peng
669 et al., 2019; Xu et al., 2023) have focused on learning within the support of the offline data, avoiding
670 OOD evaluation and improving stability. Our approach integrates multi-agent value decomposition
671 into this paradigm, ensuring more stable and coordinated policy learning in multi-agent settings.
672672 **B.2 MULTI-AGENT REINFORCEMENT LEARNING**
673674 A key challenge in MARL is the joint action space (Hernandez-Leal et al., 2019), which grows
675 exponentially with the number of agents, making it difficult to find optimal policies. The Centralized
676 Training with Decentralized Execution (CTDE) framework (Kraemer & Banerjee, 2016; Oliehoek
677 et al., 2008; Sunehag et al., 2017) addresses this by training agents centrally with global information,
678 while they execute based on decentralized policies using only local observations.
679680 Recent offline MARL approaches (Jiang & Lu, 2023; Pan et al., 2022; Shao et al., 2024; Wang
681 et al., 2024; 2023; Yang et al., 2021; Zhu et al., 2025; Liu et al., 2024; Bui et al., 2024), extend
682 online MARL methods with regularization to avoid OOD actions. For instance, ICQ (Yang et al.,
683 2021) uses importance sampling for local policy constraints, while OMAR (Pan et al., 2022) adapts
684 conservative Q-learning. In contrast to value decomposition methods, which adhere to the IGM
685 principle, AlberDice (Matsunaga et al., 2023) and ComaDice (Bui et al., 2024) employ stationary
686 distribution shift regularization to combat the distribution shift issue. MADiff (Zhu et al., 2025) uses
687 an attention-based diffusion model to effectively model agent collaboration. InSPO (Liu et al., 2024)
688 sequentially optimizes agent policies in an in-sample manner. MACCA (Wang et al., 2023) and
689 OMIGA (Wang et al., 2024) introduce global-to-local value regularization. However, these methods
690 apply a fixed conservatism level for each agent, which can be inefficient. Although CFCQL (Shao
691 et al., 2024) incorporates conservative value estimation, it fails to account for the heterogeneous
692 impact of individual agents on overall system performance. Our algorithm addresses the above
693 problems by dynamically adjusting conservative degree based on each agent’s impact on the system.
694695 **C PROOFS**
696697 **Proposition 3.1** *In an offline MARL setting, the optimal global policy $\pi_{tot}^*(a | o)$ is given by Eq. (4)*
698 *and is formally expressed as follows:*

699
$$\pi_{tot}^*(a | o) = \pi_b(a | o) \cdot \exp \left(\frac{1}{\alpha} (Q^*(o, a) - V^*(o)) \right), \quad (26)$$

700

701 *where $Q^*(o, a)$ is optimal action-value function, $V^*(o)$ is the optimal value function, and we assume
702 there is a global conservatism level α that controls the overall deviation from the behavior policy.*

702 *Proof.* The proof follows (Yang et al., 2021) and is the extension of SAC(Haarnoja et al., 2018) into
 703 offline multi-agent setting.

704 Let us return to the definition of offline MARL with regularization, we start with the original form:

$$\begin{aligned} 706 \quad & \max_{\pi_{tot}} E_{a \sim \pi_{tot}} [Q_{tot}(o, a)], \\ 707 \quad & \text{s.t. } D_{KL}(\pi_{tot} \parallel \pi_b) \leq \epsilon, \quad \sum_a \pi_{tot}(a \mid o) = 1. \end{aligned} \quad (27)$$

708 We find that the objective is a linear function of the decision variables π_{tot} and all constraints are
 709 convex functions. Thus Eq. (27) is a convex optimization problem. The Lagrangian equation is:
 711

$$\begin{aligned} 712 \quad \mathcal{L}(\pi_{tot}, \alpha, \lambda) = & \mathbb{E}_{a \sim \pi_{tot}} [Q_{tot}(o, a)] + \alpha (\epsilon - D_{KL}(\pi_{tot} \parallel \pi_b)) \\ 713 \quad & + \lambda \left(1 - \sum_a \pi_{tot}(a \mid o) \right), \end{aligned} \quad (28)$$

717 where α denotes the Lagrangian coefficient which is a global conservatism level that controls the
 718 overall deviation from the behavior policy. Then we can get the following formula:
 719

$$720 \quad \frac{\partial \mathcal{L}}{\partial \pi_{tot}} = Q_{tot}(o, a) - \alpha \left(1 + \log \left(\frac{\pi_{tot}(a \mid o)}{\pi_b(a \mid o)} \right) \right) - \lambda. \quad (29)$$

723 Setting $\frac{\partial \mathcal{L}}{\partial \pi_{tot}}$ to zero, then:
 724

$$725 \quad Q_{tot}(o, a) - \alpha \left(1 + \log \left(\frac{\pi_{tot}(a \mid o)}{\pi_b(a \mid o)} \right) \right) - \lambda = 0, \quad (30)$$

$$728 \quad Q_{tot}(o, a) = \alpha \left(1 + \log \left(\frac{\pi_{tot}(a \mid o)}{\pi_b(a \mid o)} \right) \right) + \lambda, \quad (31)$$

$$731 \quad \frac{Q_{tot}(o, a)}{\alpha} - \frac{\lambda}{\alpha} - 1 = \log \left(\frac{\pi_{tot}(a \mid o)}{\pi_b(a \mid o)} \right), \quad (32)$$

$$735 \quad \pi_{tot}(a \mid o) = \pi_b(a \mid o) \exp \left(\frac{Q_{tot}(o, a)}{\alpha} - 1 - \frac{\lambda}{\alpha} \right). \quad (33)$$

737 The optimal policy is expressed similar to Eq.(33) while adding optimal symbol to all functions,
 738 which is π to π^* . Integrating Eq.(33) with optimal symbol into the expression of optimal V-function
 739 in offline MARL with regularization, we can get:
 740

$$\begin{aligned} 741 \quad V_{tot}^*(o) &= \sum_a \pi_{tot}^*(a \mid o) \left(Q_{tot}^*(o, a) - \alpha \log \left(\frac{\pi_{tot}^*(a \mid o)}{\pi_b(a \mid o)} \right) \right) \\ 742 \quad &= \sum_a \pi_{tot}^*(a \mid o) (\lambda^* + \alpha) \\ 743 \quad &= \lambda^* + \alpha. \end{aligned} \quad (34)$$

747 Through Eq.(33) with optimal symbol and Eq.(34), we can finally obtain the optimal global policy
 748 $\pi_{tot}^*(a \mid o)$:

$$750 \quad \pi_{tot}^*(a \mid o) = \pi_b(a \mid o) \cdot \exp \left(\frac{1}{\alpha} (Q^*(o, a) - V^*(o)) \right). \quad (35)$$

751 \square

752 **Theorem.3.3** Given Eq. (23), the optimal policy for each agent is derived, and consistency between
 753 the local optimal policies π_i^* and the global optimal policy π_{tot}^* is guaranteed. This consistency holds
 754 for individual α_i assignments across agents.

756 *Proof.* To provide the proof, we initially return to the decomposition framework of the Q-function in
 757 MARL setting, which is:
 758

$$759 \quad Q(o, a) = Q_{tot}^r(o, a) + \sum_{i=1}^N \alpha_i \cdot Q^{c,i}(o, a). \quad (36)$$

$$760$$

$$761$$

762 In this decomposition framework, the global Q is divided into two parts: Q_{tot}^r represents the
 763 computation of the return, and $Q^{c,i}$ serves as the global mapping of each agent's conservatism level.
 764

765 Consider a global perspective that a global α_{tot} controls the whole conservatism level:
 766

$$766 \quad Q(o, a) = Q_{tot}^r(o, a) + \alpha_{tot} \cdot Q_{tot}^c(o, a). \quad (37)$$

$$767$$

768 Compare Eq.(36) with Eq.(37), the computation of the return is the same, while the deviation part
 769 varies due to the conservatism level. These two equations implicitly indicate that:
 770

$$771 \quad \alpha_{tot} \cdot Q_{tot}^c(o, a) = \sum_{i=1}^N \alpha_i \cdot Q^{c,i}(o, a). \quad (38)$$

$$772$$

$$773$$

774 Back to the definition of $Q^{c,i}$ and Q_{tot}^c , According to Eq.(38), we have:
 775

$$776 \quad \alpha_{tot} \cdot \log \left(\frac{\pi_{tot}^*(a | o)}{\pi_b(a | o)} \right) = \sum_i \alpha_i \cdot \log \left(\frac{\pi_i^*(a_i | o_i)}{\pi_b(a_i | o_i)} \right). \quad (39)$$

$$777$$

778 Then we separate the parts involving Q-function and V-function from the parts involving π in Eq.(26):
 779

$$780 \quad \frac{\pi_{tot}^*(a | o)}{\pi_b(a | o)} = \exp \left(\frac{1}{\alpha_{tot}} (Q^*(o, a) - V^*(o)) \right), \quad (40)$$

$$781$$

$$782$$

$$783 \quad \log \left(\frac{\pi_{tot}^*(a | o)}{\pi_b(a | o)} \right) = \frac{1}{\alpha_{tot}} (Q^*(o, a) - V^*(o)), \quad (41)$$

$$784$$

$$785$$

$$786 \quad \alpha_{tot} \cdot \log \left(\frac{\pi_{tot}^*(a | o)}{\pi_b(a | o)} \right) = Q^*(o, a) - V^*(o). \quad (42)$$

$$787$$

$$788$$

789 Similarly, the local parts in Eq.(23) can be written as :
 790

$$791 \quad \alpha_i \cdot \log \left(\frac{\pi_i^*(a_i | o_i)}{\pi_b(a_i | o_i)} \right) = w_i^r(\mathbf{o}) \left(Q_i^{r*}(o_i, a_i) - V_i^{r*}(o_i) \right) + \alpha_i \cdot \left(Q^{c,i*}(\mathbf{o}, a) - V^{c,i*}(\mathbf{o}) \right). \quad (43)$$

$$792$$

$$793$$

$$794$$

795 With Eq.(13) - (16), we can sum both sides of Eq.(43) with respect to i :
 796

$$797 \quad \sum_i \alpha_i \cdot \log \left(\frac{\pi_i^*(a_i | o_i)}{\pi_b(a_i | o_i)} \right) = \sum_i w_i^r(\mathbf{o}) \left(Q_i^{r*}(o_i, a_i) - V_i^{r*}(o_i) \right) + \sum_i \alpha_i \cdot \left(Q^{c,i*}(\mathbf{o}, a) - V^{c,i*}(\mathbf{o}) \right), \quad (44)$$

$$798$$

$$799$$

$$800$$

$$801$$

$$802$$

$$803 \quad \alpha_{tot} \cdot \log \left(\frac{\pi_{tot}^*(a | o)}{\pi_b(a | o)} \right) = \sum_i w_i^r(\mathbf{o}) \left(Q_i^{r*}(o_i, a_i) - V_i^{r*}(o_i) \right) + \sum_i \alpha_i \cdot \left(Q^{c,i*}(\mathbf{o}, a) - V^{c,i*}(\mathbf{o}) \right), \quad (45)$$

$$804$$

$$805$$

$$806$$

$$807$$

$$808 \quad \alpha_{tot} \cdot \log \left(\frac{\pi_{tot}^*(a | o)}{\pi_b(a | o)} \right) = Q^*(o, a) - V^*(o). \quad (46)$$

$$809$$

810 The transformation from Eq.(44) to Eq.(46) implies that with Eq.(23):
 811

$$812 \quad 813 \quad \pi_{tot}^*(a | o) = \prod_{i=1}^N \pi_i^*(a_i | o_i), \\ 814$$

815 which means Eq.(23) not only allows for the derivation of the optimal policy for each agent, but also
 816 ensures consistency between the local optimal policies π_i^* and the global optimal policy π_{tot}^* , even
 817 when each agent has a distinct α_i .
 818 \square
 819

820 **Proposition 3.4** *From Eq. (24), each agent's conservatism-based value function V_i^c is updated
 821 through the following optimization:*
 822

$$823 \quad 824 \quad \min_{V_i^c} \mathbb{E}_{(o_i, a_i) \sim \mathcal{D}} \left[\exp \left(\frac{w_i^r(\mathbf{o})}{\alpha_i} (Q_i^r(o_i, a_i) - V_i^r(o_i)) \right. \right. \\ 825 \quad \left. \left. + (Q^{c,i}(o, a) - V^{c,i}(o)) \right) + \frac{w_i^r(\mathbf{o}) V_i^r(o_i) + \alpha_i V^{c,i}(o)}{\alpha_i} \right]. \quad (47)$$

826 The proof (similar to (Wang et al., 2024)) follows by showing that the first-order optimal
 827 condition of the above optimization objective, where the derivative with respect to $V^{c,i}$ equals zero,
 828 is exactly the Eq.(24):
 829

$$830 \quad 831 \quad \frac{\partial}{\partial V^{c,i}(o)} \left[\exp \left(\frac{w_i^r(\mathbf{o})}{\alpha_i} (Q_i^r(o_i, a_i) - V_i^r(o_i)) \right. \right. \\ 832 \quad \left. \left. + (Q^{c,i}(o, a) - V^{c,i}(o)) \right) + \frac{w_i^r(\mathbf{o}) V_i^r(o_i) + \alpha_i V^{c,i}(o)}{\alpha_i} \right] = 0 \quad (48)$$

$$833 \quad \Rightarrow \quad 834 \quad \mathbb{E}_{a_i \sim \pi_b} \left[-\exp \left(\frac{w_i^r(\mathbf{o})}{\alpha_i} (Q_i^r(o_i, a_i) - V_i^r(o_i)) \right. \right. \\ 835 \quad \left. \left. + (Q^{c,i}(o, a) - V^{c,i}(o)) \right) + 1 \right] = 0. \quad (49)$$

836 From the perspective of seeking the optimal function, we can have:
 837

$$838 \quad 839 \quad \mathbb{E}_{a_i \sim \pi_b} \left[\exp \left(\frac{w_i^r(\mathbf{o})}{\alpha_i} (Q_i^{r^*}(o_i, a_i) - V_i^{r^*}(o_i)) \right. \right. \\ 840 \quad \left. \left. + (Q^{c,i^*}(\mathbf{o}, a) - V^{c,i^*}(\mathbf{o})) \right) \right] = 1. \quad (50)$$

841 This result implies that the optimal form of V_i^c can be obtained by solving the convex optimization
 842 problem in Eq.(47).
 843 \square

844 D EXPERIMENT SETTINGS

845 We select **Multi-Agent MuJoCo**(de Witt et al., 2020) and the **StarCraft Multi-Agent Challenge**
 846 (**SMAC**)(Samvelyan et al., 2019) as our experimental environments.
 847

848 Multi-Agent MuJoCo, a benchmark for continuous multi-agent robotic control, is built on the MuJoCo
 849 environment. The Multi-Agent MuJoCo dataset we use was collected using the HAPPO(Kuba et al.,
 850

2021) algorithm by (Wang et al., 2024) which contains four quality levels: expert, medium, medium-replay and medium-expert. The expert dataset is generated by employing the converged HAPPO algorithm, which involves training the algorithm until it reaches a state of convergence, where the agents have learned optimal policies. The medium dataset is generated by first training a policy online using HAPPO, early-stopping the training, and collecting samples from this partially-trained policy. The medium-replay dataset consists of recording all samples in the replay buffer observed during training until the policy reaches the medium level of performance. The medium-expert dataset is constructed by mixing equal amounts of expert demonstrations and suboptimal data. For all datasets, the hyperparameter `env_args.agent_obs` is set to 1. The average returns of the datasets are listed in Table 2.

Table 2: The multi-agent MuJoCo datasets.

Scenario	Quality	Average Return
2-Agent Ant	expert	2055.07
2-Agent Ant	medium	1418.70
2-Agent Ant	medium-expert	1736.88
2-Agent Ant	medium-replay	1029.51
3-Agent Hopper	expert	2452.02
3-Agent Hopper	medium	723.57
3-Agent Hopper	medium-expert	1190.61
3-Agent Hopper	medium-replay	746.42
6-Agent HalfCheetah	expert	2785.10
6-Agent HalfCheetah	medium	1425.66
6-Agent HalfCheetah	medium-expert	2105.38
6-Agent HalfCheetah	medium-replay	655.76

The second environment, SMAC, is a widely-used benchmark for evaluating cooperative MARL methods. SMAC consists of a set of StarCraft II micro scenarios, and all scenarios are confrontations between two groups of units. Agents based on the MARL algorithm control the first group’s units, while a built-in heuristic game AI bot with different difficulties controls the second group’s units. Scenarios vary in terms of the initial location, number and type of units, and elevated or impassable terrain. The available actions for each agent include no operation, move[direction], attack [enemy id], and stop. The reward that each agent receives is the same. The hit-point damage dealt and received determines the agents’ share of the reward. The offline SMAC dataset is collected by (Meng et al., 2021), using online-trained MAPPO(Kuba et al., 2021) agents. This is the largest publicly available dataset for SMAC and includes three quality levels: good, medium, and poor. We focus on three representative battle maps in our experiments: one hard map (5m_vs_6m) and two super hard maps (6h_vs_8z and corridor). The task types of the maps are listed in the Table 3. For each dataset in a map, we randomly sample 1000 episodes as our dataset. The average returns of SMAC datasets are listed in Table 4.

Table 3: SMAC maps for experiments.

Map Name	Type
5m_vs_6m	homogeneous & asymmetric
6h_vs_8z	micro-trick: focus fire
corridor	micro-trick: wall off

E IMPLEMENTATION DETAILS

E.1 ALGORITHM SUMMARY

In this section, we will give an explanation of the pseudocode for OMCDA. The pseudocode is shown in Algorithm. 1 We initialize the **behavior policy** π_b through behavior cloning (Michie et al.,

918
919
920
921
922
923
924
925
926
927
928
929
930

Table 4: The SMAC datasets.

Map Name	Quality	Average Return
5m_vs_6m	good	20.00
5m_vs_6m	medium	11.03
5m_vs_6m	poor	8.50
6h_vs_8z	good	17.84
6h_vs_8z	medium	11.96
6h_vs_8z	poor	9.12
corridor	good	19.88
corridor	medium	13.07
corridor	poor	4.93

Algorithm 1 Pseudocode of OMCDA

Input: Offline dataset D, d_{tot}
 Initialize return-based state-value network V_i^r , constraint-based state-value network V_i^c , return-based action-value network Q_i^r , constraint-based action-value network Q_i^c , conservatism level α_i , and policy network π_i for agent $i = 1, 2, \dots, n$.

for $t = 1$ **to** max-step **do**

- Sample batch transitions (o, a, r, o') from D .
- Update return-based state-value function $V_i^r(o)$ for each agent i , via Eq. (51).
- Update constraint-based state-value function $V_i^c(o)$ for each agent i , via Eq. (25).
- Compute $V_{tot}^r(o')$ and $Q_{tot}^r(o, a)$, via Eq. (15) and Eq. (13).
- Update return-based action-value network $Q_i^r(o, a)$, via Eq. (53).
- Update constraint-based action-value network $Q_i^c(o, a)$, via Eq. (52).
- Update local policy network π_i for each agent i , via Eq. (54).
- Calculate m_i with Eq.(19) and update each agent's conservative degree d_i , via Eq. (17).
- Update each agent's conservatism level α_i , via Eq. (55).

end for

947

1990) using the offline dataset. The procedure begins by initializing all necessary networks and parameters for each agent. At each iteration, the algorithm samples transitions from the dataset D and performs sequential updates of both local and global networks.

951
952
953

1. State-Value Updates: The state-value functions V_i^r and V_i^c are updated first. Inspired by IQL(Kostrikov et al., 2021b) , we can implicitly update V_i^r by leveraging the expectile loss, thus avoiding the use of out-of-distribution data. V_i^r and V_i^c are updated as following:

954
955
956

Update V_i^r : The return-based state-value function $V_i^r(o)$ for each agent is updated by minimizing the following objective:

957
958

$$\min_{V_i^r} \mathbb{E}_{(o_i, a_i) \sim \mathcal{D}} [L_2^\tau (Q_i^r(o_i, a_i) - V_i^r(o_i))], \quad (51)$$

959
960

where L_2^τ denotes the expectile loss with parameter τ , balancing the updates based on the agent's value estimation errors.

961
962

Update V_i^c : The constraint-based state-value function $V_i^c(o)$ is updated using Eq.(25).

963
964

2. Global Value Computation: In this step, we compute the global term for return-based function. Here $V_{tot}^r(o')$ and $Q_{tot}^r(o, a)$ are calculated in Eq.(15) and Eq.(13).

965
966
967

3. Action-Value Updates: Each agent's action-value networks Q_i^r and Q_i^c are then updated. This step ensures that the agents maintain the correct mapping between their actions and the expected return as well as conservatism constraints.

968
969
970
971

Update Q_i^c : The constraint-based action-value function Q_i^c , along with the weight $w^{c,i}$ and bias $b^{c,i}$, is updated by minimizing the following objective, while $Q^{c,i}$ and $V^{c,i}$ are from Eq.(14) and Eq.(16):

$$\min_{Q_i^c, w^{c,i}, b^{c,i}} \mathbb{E}_{(\mathbf{o}, \mathbf{a}, \mathbf{o}') \sim \mathcal{D}} \left[(Q^{c,i}(\mathbf{o}, \mathbf{a}) - \gamma V^{c,i}(\mathbf{o}'))^2 \right]. \quad (52)$$

972 **Update Q_i^r :** The return-based action-value function Q_i^r , weight w_i^r , and bias b^r are updated according
 973 to the following minimization objective:
 974

$$975 \min_{\substack{Q_i^r, w_i^r, b^r \\ i=1, \dots, n}} \mathbb{E}_{(\mathbf{o}, \mathbf{a}, \mathbf{o}') \sim \mathcal{D}} \left[(r(\mathbf{o}, \mathbf{a}) + \gamma V_{tot}^r(\mathbf{o}') - Q_{tot}^r(\mathbf{o}, \mathbf{a}))^2 \right]. \quad (53)$$

978 **4. Policy Updates:** The agent's policy network is updated based on optimizing the following function.
 979

980 **Update π_i :** The policy π_i for each agent is updated by enforcing the KKT condition on Eq.(5)
 981 leveraging Eq.(22):
 982

$$983 \max_{\pi_i} \mathbb{E}_{(o_i, a_i) \sim \mathcal{D}} \left[\exp \left(\frac{w_i^r(\mathbf{o})}{\alpha_i} (Q_i^r(o_i, a_i) - V_i^r(o_i)) \right. \right. \\ 984 \left. \left. + (Q^{c,i}(o, a) - V^{c,i}(o)) \right) \cdot \log \pi_i(a_i | o_i) \right]. \quad (54)$$

985 **5. Conservatism Updates:** Finally, each agent's conservative degree d_i is updated to ensure the
 986 balance between the risk and flexibility for each agent. After calculate m_i with Eq.(19), we can
 987 update d_i following Eq.(17). While the conservatism level α_i is adjusted to control the balance
 988 between deviation and conservatism.
 989

990 **Update α_i :** The conservatism level α_i is updated according to Eq.(55).
 991

$$992 \min_{\alpha_i} \mathbb{E}_{(o_i, a_i) \sim \mathcal{D}} \left[\alpha_i \cdot d_i - \alpha_i \cdot D_{KL}(\pi_i \| \pi_b^i) \right]. \quad (55)$$

993 If the deviation from the behavior policy is less than d_i , α_i will decrease, allowing more flexibility
 994 for exploration. Conversely, if the deviation exceeds d_i , α_i will increase, pushing the policy to stay
 995 closer to the behavior policy.
 996

1001 E.2 DETAILS OF OMCDA

1002 The return-computation and constraint modules in the Q-function and V-function, and policy networks
 1003 of OMCDA are represented by 3-layer ReLU activated MLPs with 256 units for each hidden layer.
 1004 For the both weight networks of the two modules, we use 2-layer ReLU-activated MLPs with 64
 1005 units for each hidden layer. All the networks are optimized by Adam optimizer.
 1006

1007 For the computation of the influence term, in practice, directly computing the derivatives can indeed
 1008 lead to numerical instability. Therefore, we employ several techniques to stabilize the differentiation
 1009 process: For continuous action spaces such as MuJoCo, we adopt a reparameterization method
 1010 and use single-sample average for obtaining expectations for algorithm stability, simplifying the
 1011 original differentiation process into a relationship between Q^r and the log variance of policy network,
 1012 which is then directly computed using deep learning libraries in PyTorch. For discrete action space
 1013 environments like SMAC, due to the finite action set, we approximate the target derivative by applying
 1014 small parameter perturbations to π and using finite difference approximation trick.
 1015

1016 In this paper, all experiments are implemented with Pytorch and executed on NVIDIA A100 GPUs.
 1017

1018 E.3 DETAILS OF BASELINES AND COMPARATIVE EVALUATION

1019 We compare our approach with seven recent offline MARL algorithms: The multi-agent versions of
 1020 BCQ(Fujimoto et al., 2019) and CQL(Kostrikov et al., 2021b) (referred to as BCQ-MA and CQL-
 1021 MA), ICQ(Yang et al., 2021), OMAR(Pan et al., 2022), CFCQL (Shao et al., 2024), OMIGA(Wang
 1022 et al., 2024), and ComaDICE(Bui et al., 2024). Both BCQ-MA and CQL-MA utilize a linear
 1023 weighted value decomposition structure for the multi-agent setting, similar to Eq. (1).
 1024

1025 Table 6 and Table 7 presents the mean and standard deviation of average returns for the offline
 1026 Multi-Agent MuJoCo and SMAC tasks with 5 random seeds. In these multi-agent scenarios, the
 1027 complexity of the environment makes it challenging to assign conservative degree to individual agents,
 1028

1026 as different agents' deviations from their behavior policies have varying impacts on the environment,
 1027 which in turn influences the learning process. The dynamic conservative degree allocation mechanism
 1028 in OMCDA assigns different conservatism levels to each agent based on their varying impacts on
 1029 the system, which leads to better overall system performance. Moreover, by separating the return
 1030 optimization from policy deviation management, OMCDA provides a more refined learning process,
 1031 resulting in improved stability and effectiveness, enabling better collaboration and more efficient
 1032 policy learning compared to other offline MARL methods.

Table 5: Hyper-parameter of OMCDA.

Hyperparameter	Value
OMCDA	
Value network for return learning rate	2e-4
Value network for constraint learning rate	4e-5
Alpha learning rate	1e-5
Policy network learning rate	2e-4
Optimizer	Adam
Target update rate	0.005
Batch size	128
Discount factor	0.99
Hidden dimension	256
Expectile parameter τ	0.7
Initial conservative degree d_i	0.05 or 0.1 or 0.2

E.4 HYPERPARAMETERS

For multi-agent MuJoCo and SMAC, the hyperparameters of OMCDA are listed in Table 5. Since we aim to quickly learn the return while maintaining stability in deviation, we use different learning rates for the value network: one for return and another for the constraint, set to 2×10^{-4} and 4×10^{-5} , respectively. In OMCDA, the conservative degree d is an important parameter. When the value of d is large, the algorithm's overall conservative degree increases, providing the system with greater flexibility in policy exploration. Conversely, when the conservative degree is smaller, the policy tends to align more closely with the behavior policy. In the multi-agent MuJoCo environment, for the expert dataset, we set the initial $d_i = 0.05$ for each agent to guarantee effective regularization, while for other datasets, we set the initial $d_i = 0.2$ to maintain moderate deviation. In the SMAC environment, for the good dataset, we set the initial $d_i = 0.1$ for each agent, and $d_i = 0.2$ for the other datasets.

E.5 DETAILS OF EQ. (5)

Consider a common case where there's only a global constraint:

$$\max_{\pi} E \left[\sum_{t=0}^{\infty} \gamma^t r_t \right], \text{ s.t. } E_{a \sim \pi} \left[\log \frac{\pi_t(a_t | o_t)}{\pi_b(a_t | o_t)} \right] \leq d_{tot}. \quad (56)$$

Then according to the Lagrangian relaxation, the global conservatism level α_{tot} can be assigned and the Q-function is formulated as:

$$Q(o, a) = \mathbb{E} \left[\sum_{t=0}^{\infty} \gamma^t (r_t - \alpha_{tot} \cdot D_{\text{KL}}(\pi_t \| \pi_b)) \right]. \quad (57)$$

When considering Eq. (56) under the constraints specified in Eq. (5) and Proposition 3.2, the global constraint can be transformed step by step:

$$E_{a \sim \pi} \left[\log \frac{\pi_t(a_t | o_t)}{\pi_b(a_t | o_t)} \right] \leq d_{tot}, \quad (58)$$

1080

1081

1082

1083

1084

1085

1086

1087

1088

1089

1090

1091

1092

1093

1094

1095

1096

1097

1098

1099

1100

1101

1102

1103

1104

1105

1106

1107

1108

1109

1110

1111

1112

1113

Table 6: Offline Multi-agent MuJoCo Tasks

Multi-agent MuJoCo									
Task	Dataset	BCQ-MA	CQL-MA	ICQ	OMAR	CFCQL	OMIGA	ComaDICE	OMCDA
Hopper	expert	77.85±58.04	159.14±313.83	754.74±806.28	2.36±1.46	802.33±544.89	859.63±709.47	2827.7±62.9	1214.25±830.72
Hopper	medium	44.58±20.62	401.27±199.88	501.79±14.03	21.34±24.90	389.75±105.67	1189.26±544.30	822.6±66.2	1441.53±488.91
Hopper	m-replay	26.53±24.04	31.37±15.16	195.39±103.61	3.30±3.22	567.54±453.65	774.18±494.27	906.3±242.1	1733.27±379.71
Hopper	m-expert	54.31±23.66	64.82±123.31	355.44±373.86	1.44±0.86	721.23±342.56	709.00±595.66	1362.4±522.9	1047.13±523.67
Ant	expert	1317.73±286.28	1042.39±2021.65	2050.00±11.86	312.54±297.48	1987.98±34.65	2055.46±1.58	2056.9±5.9	2056.95±6.43
Ant	medium	1059.60±91.22	535.90±1766.42	1412.41±10.93	-1710.04±1588.98	1406.56±123.59	1418.44±5.36	1425.0±2.9	1376.03±141.55
Ant	m-replay	950.77±48.76	234.62±1618.28	1016.68±53.51	-2014.20±844.68	854.41±128.98	1105.13±88.87	1122.9±61.0	1142.59±75.15
Ant	m-expert	1020.89±242.74	800.22±1621.52	1590.18±85.61	-2992.80±6.95	978.87±65.45	1720.33±110.63	1813.9±68.4	1988.09±41.49
HalfCheetah	expert	2992.71±629.65	1189.54±1034.49	2955.94±459.19	-206.73±161.12	2399.12±345.65	3383.61±552.67	4082.9±45.7	4963.92±126.69
HalfCheetah	medium	2590.47±110.35	1011.35±1016.94	2549.27±96.34	-265.68±146.98	1845.43±76.78	3608.13±237.37	2664.7±54.2	3883.60±93.43
HalfCheetah	m-replay	-333.64±152.06	1998.67±693.92	1922.42±612.87	-235.42±154.89	1766.45±659.78	2504.70±83.47	2855.0±242.2	2993.03±271.84
HalfCheetah	m-expert	3543.70±780.89	1194.23±1081.06	2839.93±924.02	-253.84±63.94	1934.23±867.43	2948.46±518.89	3889.7±81.6	4483.76±268.71

$$\sum_i E_{a \sim \pi} \left[\log \frac{\pi_t^i(a_t^i | o_t^i)}{\pi_b(a_t^i | o_t^i)} \right] \leq \sum_i d_i, \quad (59)$$

$$E_{a \sim \pi} \left[\log \frac{\pi_t^i(a_t^i | o_t^i)}{\pi_b(a_t^i | o_t^i)} \right] \leq d_i, \quad \sum_i d_i = d_{tot}, \quad \forall i = 1 \dots n. \quad (60)$$

Therefore, we effectively achieve an equivalent transformation from global to local policy constraints. By comparing the Q-function under the global constraint in Eq. (57) with that under local constraints in Eq. (6), and noting that $E_{a \sim \pi} \left[\log \frac{\pi_t^i(a_t^i | o_t^i)}{\pi_b(a_t^i | o_t^i)} \right] = E_{a_i \sim \pi_i} \left[\log \frac{\pi_t^i(a_t^i | o_t^i)}{\pi_b(a_t^i | o_t^i)} \right]$, the following conclusion can be derived from this equivalence:

$$Q(o, a) = \mathbb{E} \left[\sum_{t=0}^{\infty} \gamma^t (r_t - \alpha_{tot} \cdot D_{KL}(\pi_t \| \pi_b)) \right] = \mathbb{E} \left[\sum_{t=0}^{\infty} \gamma^t \left(r_t - \sum_i \alpha_i \cdot D_{KL}(\pi_t^i \| \pi_b) \right) \right], \quad (61)$$

$$\alpha_{tot} \cdot \log \left(\frac{\pi(a | o)}{\pi_b(a | o)} \right) = \sum_i \alpha_i \cdot \log \left(\frac{\pi_i(a_i | o_i)}{\pi_b(a_i | o_i)} \right). \quad (62)$$

Eq. (62) effectively decomposes the global deviation term into local components, thereby establishing the foundation for both generating Eq. (38) and the deviation term in Eq. (12).

Table 7: Offline SMAC Tasks

SMAC									
Task	Dataset	BCQ-MA	CQL-MA	ICQ	OMAR	CFCQL	OMIGA	ComaDICE	OMCDA
5m_vs_6m	good	7.76±0.15	8.08±0.21	7.87±0.30	7.40±0.63	8.13±0.32	8.25±0.37	8.7±0.5	10.47±0.24
5m_vs_6m	medium	7.58±0.10	7.78±0.10	7.77±0.30	7.08±0.51	7.55±0.36	7.92±0.57	8.7±0.4	10.19±0.15
5m_vs_6m	poor	7.61±0.36	7.43±0.10	7.26±0.19	7.27±0.42	7.49±0.12	7.52±0.21	8.1±0.5	9.57±0.18
corridor	good	15.24±1.21	5.22±0.81	15.54±1.12	6.74±0.69	14.25±0.78	15.88±0.89	18.0±0.1	14.72±0.60
corridor	medium	10.82±0.92	7.04±0.66	11.30±1.57	7.26±0.71	11.44±1.32	11.66±1.30	12.9±0.6	13.06±0.71
corridor	poor	4.47±0.94	4.08±0.60	4.47±0.43	4.28±0.49	4.89±0.37	5.61±0.35	6.4±0.5	6.54±0.51
6h_vs_8z	good	12.19±0.23	10.44±0.20	11.81±0.12	9.85±0.28	11.87±1.25	12.54±0.21	13.1±0.5	14.14±0.21
6h_vs_8z	medium	11.77±0.16	11.29±0.29	11.13±0.33	10.36±0.16	12.25±0.43	12.19±0.22	12.8±0.2	13.65±0.31
6h_vs_8z	poor	10.84±0.16	10.81±0.52	10.55±0.10	10.63±0.25	10.89±0.47	11.31±0.19	11.4±0.6	10.83±0.10

F ADDITIONAL RESULTS

F.1 ANALYSIS ON THE COMPONENTS OF OMCDA

To analyze the solution to conservative degree allocation and assess the impact of Q-function decomposition in OMCDA, we conduct three distinct ablation studies: OMCDA-w/o-CDA, OMCDA-w/o-dq, and OMCDA-rd. In OMCDA-w/o-CDA, all agents are assigned the same conservative degree d_i , without the implementation of conservative degree allocation. In contrast, OMCDA-w/o-dq maintains the dynamic conservative degree allocation but eliminates the Q-function decomposition, preventing the separation of return optimization from policy deviation handling. OMCDA-rd introduces random allocation of the conservatism constraint, assigning each agent a random d_i , in which we hope to evaluate the importance of strategically assigning conservatism levels based on each agent's impact.

Experiments are conducted on the HalfCheetah and 6h_vs_8z tasks in the Multi-agent MuJoCo and SMAC environments, respectively. Figure. 5 shows that OMCDA consistently outperforms all

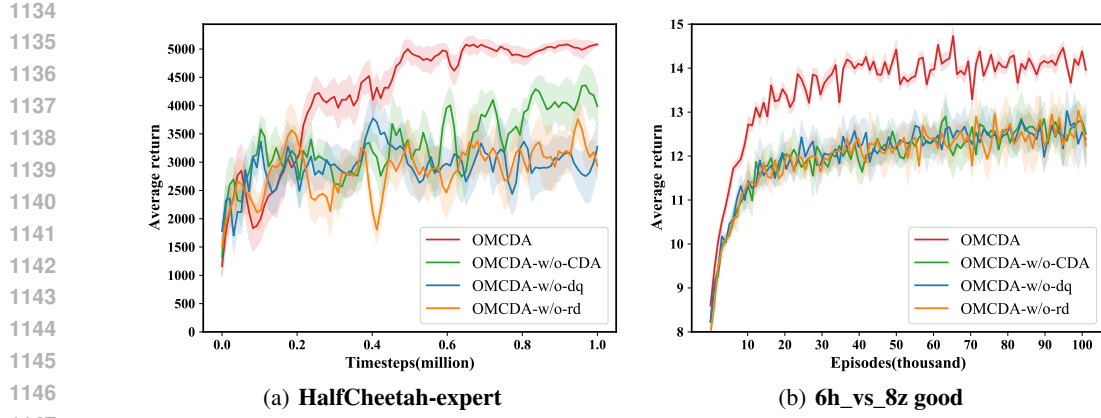


Figure 5: Analysis on the components of OMCDA

ablated versions across both tasks. In OMCDA-w/o-CDA, the absence of dynamic conservative degree allocation results in imbalanced agent behavior, with some agents being overly conservative and others overly aggressive, leading to performance degradation. OMCDA-w/o-dq exhibits weaker results due to the entanglement of return maximization and constraint handling, which complicates learning and produces suboptimal policies. OMCDA-rd, which applies random conservatism allocation, demonstrates inferior performance, as randomly assigned d_i values fail to account for each agent's unique influence on system performance.

These results confirm that both the dynamic conservative degree allocation and Q-function decomposition are essential for achieving better collaboration and learning efficiency in offline multi-agent environments, while the strategic assignment of conservatism is crucial for optimizing system performance.

F.2 ANALYSIS ON THE TOTAL CONSERVATIVE DEGREE

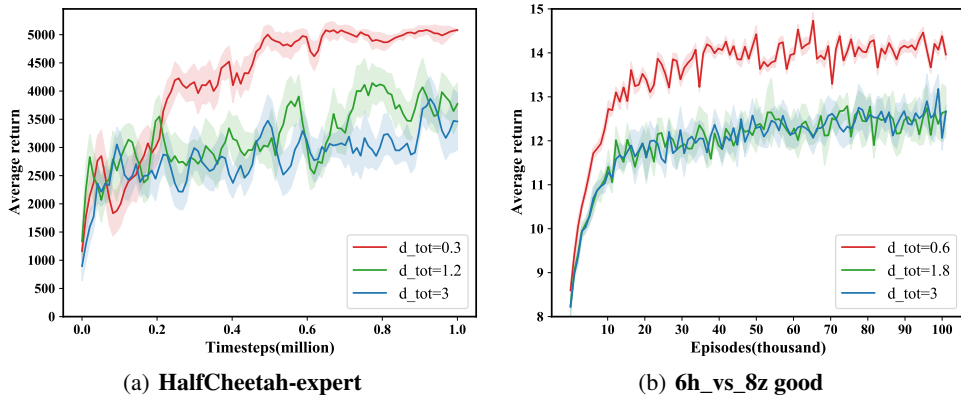


Figure 6: Analysis on the total conservative degree

The total conservative degree d_{tot} controls how much the system is permitted to deviate from the behavior policy. It establishes the total permissible deviation for the entire system, ensuring that agents do not diverge excessively from the behavior policy, helping to avoid the introduction of suboptimal actions into the system.

In our experiments on the HalfCheetah and 6h_vs_8z environments, which are based on high-quality datasets, a smaller d_{tot} outperforms the other settings. This is because, in such environments, it is essential for the policies to stay closer to the behavior policy for stable performance. At the same time, the dynamic allocation of d_i allows agents that have a significant impact on the system's return

1188 to have some flexibility to deviate, while requiring other agents to remain more conservative and
 1189 adhere closely to the behavior policy. The experimental results in Figure. 6 demonstrate that properly
 1190 adjusting d_{tot} improves system performance and allows influential agents to achieve beneficial
 1191 deviations while maintaining overall system stability.

1192

1193

1194

1195

1196

1197

1198

1199

1200

1201

1202

1203

1204

1205

1206

1207

1208

1209

1210

1211

1212

1213

1214

1215

1216

1217

1218

1219

1220

1221

1222

1223

1224

1225

1226

1227

1228

1229

1230

1231

1232

1233

1234

1235

1236

1237

1238

1239

1240

1241

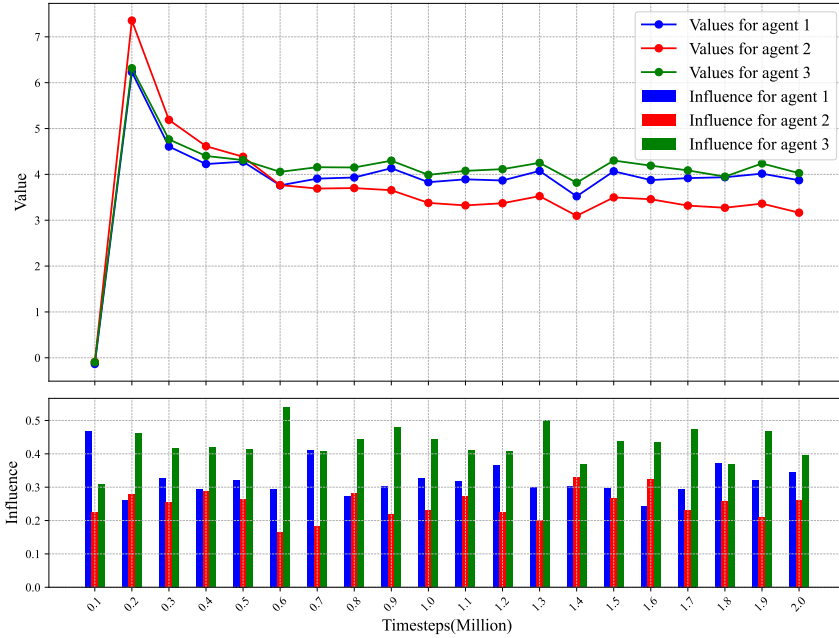


Figure 7: Analysis on the Influence Term on Hopper-medium-replay

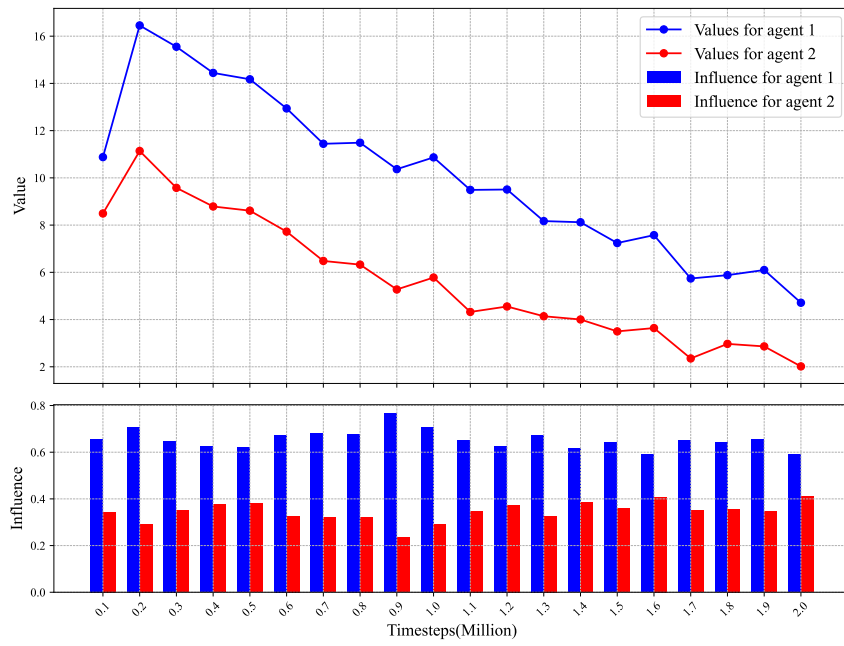


Figure 8: Analysis on the Influence Term on Ant-medium-expert

1242 F.3 ANALYSIS ON THE INFLUENCE TERM
12431244 In OMCDA, the influence of each agent on the system is the core metric for allocating conservatism
1245 levels. To determine whether we have accurately assessed each agent’s influence in the environment,
1246 we conduct experiments to analyze the relationship between the computed influence of each agent
1247 and its corresponding return.1248 The results in Figure. 7 and Figure. 8 demonstrate that agents with higher V_i^r , representing higher
1249 individual returns, tend to be allocated more influence within the system, enabling them to have a
1250 stronger impact on system-wide performance. This proportional allocation allows high-return agents
1251 to further contribute to global objectives and optimize overall system behaviour.1252 By adjusting conservatism levels properly, OMCDA enhances individual agent performance and
1253 maximizes collective system return, promoting balanced and efficient learning across all agents.
1254

1255

1256

1257

1258

1259

1260

1261

1262

1263

1264

1265

1266

1267

1268

1269

1270

1271

1272

1273

1274

1275

1276

1277

1278

1279

1280

1281

1282

1283

1284

1285

1286

1287

1288

1289

1290

1291

1292

1293

1294

1295